

Article

Local and Non-Local Invasive Measurements on Two Quantum Spins Coupled via Nanomechanical Oscillations

Dimitrios Maroulakos, Levan Chotorlishvili *, Dominik Schulz and Jamal Berakdar

Institut für Physik, Martin-Luther Universität Halle-Wittenberg, D-06120 Halle/Saale, Germany; dimitrios.maroulakos@student.uni-halle.de (D.M.); dominik.schulze@physik.uni-halle.de (D.S.); jamal.berakdar@physik.uni-halle.de (J.B.)

* Correspondence: levan.chotorlishvili@physik.uni-halle.de

Received: 24 May 2020; Accepted: 29 June 2020; Published: 1 July 2020



Abstract: Symmetry plays the central role in the structure of quantum states of bipartite (or many-body) fermionic systems. Typically, symmetry leads to the phenomenon of quantum coherence and correlations (entanglement) inherent to quantum systems only. In the present work, we study the role of symmetry (i.e., quantum correlations) in invasive quantum measurements. We consider the influence of a direct or indirect measurement process on a composite quantum system. We derive explicit analytical expressions for the case of two quantum spins positioned on both sides of the quantum cantilever. The spins are coupled indirectly to each others via their interaction with a magnetic tip deposited on the cantilever. Two types of quantum witnesses can be considered, which quantify the invasiveness of a measurement on the systems' quantum states: (i) A local quantum witness stands for the consequence on the quantum spin states of a measurement done on the cantilever, meaning we first perform a measurement on the cantilever, and subsequently a measurement on a spin. (ii) The non-local quantum witness signifies the response of one spin if a measurement is done on the other spin. In both cases the disturbance must involve the cantilever. However, in the first case, the spin-cantilever interaction is linear in the coupling constant Ω , where as in the second case, the spin-spin interaction is quadratic in Ω . For both cases, we find and discuss analytical results for the witness.

Keywords: cavity quantum electrodynamics; quantum metrology; NV center; quantum entanglement

1. Introduction

Since the foundational development of quantum mechanics, the measurement process and the wave function collapse have been under discussion [1–15]. One aspect is how to quantify and possibly modify the destructive effect of a certain measurement on a quantum state, an issue that is clearly of importance for quantum information transfer and processing. Here, we consider the “quantum witness” as the measure invasiveness in a combined quantum system. Our system described by the density operator $\hat{\rho}_{AB}$ consists of two parties A and B that interact with each other either directly $A \iff B$ or indirectly through the third quantum system f , i.e., $A \xleftrightarrow{\Omega} f \xleftrightarrow{\Omega} B$. Here, Ω is the coupling constant between f and A or B . Let us consider two types of measurements: (i) We perform a measurement on f , and then on A , in contrast to measuring A directly. (ii) We conduct a measurement on A and then on B . For Case (i), A interacts with f directly. Measurements done on f have a direct influence on the outcome of measurements done on A ; this case is referred to as the local quantum witness. In Case (ii), A and B are interrelated via f ; a measurement performed on A affects B through the quantum channel f , a case called the non-local quantum witness. One may wonder about

the outcome when the character of the channel f changes from inherently quantum to purely classical ($f_q \rightarrow f_{cl}$); the latter situation is relevant to local operations and classical communication. As discussed below, in our system, we find that the non-local quantum witness mediated through the classical channel is not zero. Specifically, we consider two nitrogen vacancy (NV) centers described by the density operator $\equiv \hat{\rho}_{AB}$ interacting via quantum modes of a nanomechanical oscillator f (see [16–53] and the references therein) with a magnetic tip attached to its end.

Wave-particle duality is a fundamental principle of quantum mechanics postulating that even macroscopic objects have wave features. However, the manifestation of quantum behavior is inversely proportional to the mass of the particle $\lambda = \frac{2\pi\hbar}{mv}$, where λ is the de Broglie wavelength, m and v are the mass and velocity of the particle, and \hbar is the Planck constant. Hence, mechanical motion, in general, should be viewed as classical unless the system is not cooled down to the temperature below $T \ll 2\pi\hbar\omega/k_B$. For example, for mode frequency $\omega = 1\text{kHz}$, the temperature should be lower than $T \ll 50\text{nK}$. Fortunately, the resonant frequency scales inversely with the size of the system. Thus, by considering nanosized cantilevers and cooling the systems to low temperature, mechanical motion switches its character and crosses the threshold boundary between the classical and quantum world. The viable technological progress of the last two decades allowed the fabrication of hybrid spin nanomechanical systems. Nanoelectromechanical resonators (NAMR) are essential for both the understanding of fundamental questions and technological applications as well. The paradigmatic model of NAMR consists of the spin of the NV center interacting with a magnetic tip. The magnetic tip is attached to the end of the nano-cantilever (i.e., cavity field). The oscillation of the cantilever modulates the spin-tip interaction and activates the spin dynamics or vice versa; the highly sensitive cantilever can detect the spin dynamics. The magnetic force between a ferromagnetic tip and NV spin implemented in magnetic resonance imaging experiments allows achieving a single-spin sensitivity and is an essential experimental scheme for NAMR [52,53]

For observing quantum behavior, the cantilever must be cooled to low temperatures to avoid thermally excited vibrations. MRFM provides tools needed to read out the cantilever and determine and possibly control its quantum state. The read out procedure on the formal mathematical language can be interpreted in terms of the phonon number projective operators (i.e., phonons are particles characterizing the quantized motion of the cantilever). We note that our model corresponds to the zero temperature case and closed quantum systems. Therefore, phenomena typical for open quantum systems, i.e., dissipation and decoherence, are beyond our project's scope. Concerning these issues, we refer to the works of Melkikh [54,55].

The spins of the NV centers are affected by a tip magnetization. In turn, the tip magnetization is strongly stabilized by intrinsic magnetic interactions (magnetic anisotropy) and hence remains basically static during the NV spin dynamics (cf. Figure 1). The quantized elastic modes of the cantilever are however decisive in that the cantilever oscillation modulates the spin-magnetic tip interaction. The modes of the cantilever are in turn modified by the coupling to the NV centers, which allows sensing the NV's spin dynamics [52,53]. The goal is to study the invasiveness of a measurement done on the quantum cantilever f (see Figure 1) for the NV spin A . In particular, we monitor the invasiveness as a function of mean "phonon number" u^2 in the coherent state and as we vary the detuning between frequencies of the NV center and cantilever mode. The paper is organized as follows: In Section 2, we specify the model. In Section 3, we present the analytical solution of the model. In Section 4, we study the invasiveness of quantum measurements done on the cantilever and NV centers.

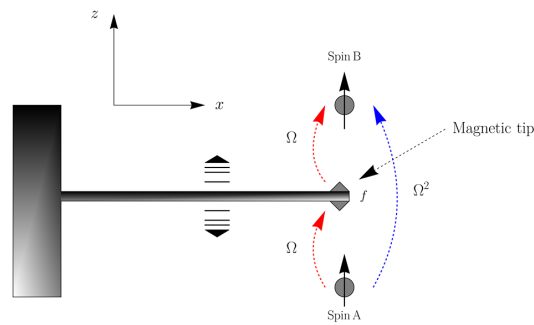


Figure 1. A schematic for the model studied in the text. The spin states of two nitrogen vacancy (NV) centers *A* and *B* interact through a magnetic tip positioned at the end of nanomechanical oscillators (cantilever). The strength of the interaction between the cantilever and NV spins is proportional to the constant Ω . The interaction between the NV center spins *A* and *B* is not direct and is proportional to Ω^2 .

2. Model

We consider two NV spins embedded in a cavity at an equal distance from the cantilever. In the general case, the Hamiltonian of the system reads [51]:

$$\begin{aligned}\hat{H} &= \hat{H}_0 + \hat{V}, \\ \hat{H}_0 &= \omega_0 (\hat{S}_1^z + \hat{S}_2^z) + \omega_f \hat{a}^\dagger \hat{a}, \\ \hat{V} &= \Omega \left\{ \hat{a}^\dagger (\hat{S}_1^- + \hat{S}_2^-) + \hat{a} (\hat{S}_1^+ + \hat{S}_2^+) \right\}.\end{aligned}\quad (1)$$

Here, Ω is the coupling constant of the NV spin with the magnetic tip, \hat{a}^\dagger , \hat{a} are the phononic creation and annihilation operators describing the cantilever oscillations with the frequency ω_f , and ω_0 is the frequency of the NV spin. For a more detailed discussion of the parameters, we refer to [51] and the references therein.

The spins' interaction with the magnetic tip \hat{V} leads to an effective indirect interaction between NV spins mediated by phonons. The experimental relevance of the model relies on the fabrication of cantilevers with frequencies comparable with the NVs' spin transition frequencies. We consider the analytical solution in the resonant and highly off-resonant cases. These two situations are distinguished by the detuning of the cantilever's oscillation with regard to the frequency of the NV spins. For strong detuning, we employ Fröhlich's method [56] to infer the effective interaction $\hat{H}_{\text{eff}}^{(1)}$ and then the effective Hamiltonian \hat{H}_{eff} :

$$\begin{aligned}\hat{H}_{\text{eff}}^{(1)} &= \frac{i}{2} \int_{-\infty}^0 d\tau [\hat{V}(\tau), \hat{V}(0)], \\ \hat{V}(t) &= \exp(-i\hat{H}_0 t) \hat{V} \exp(i\hat{H}_0 t),\end{aligned}\quad (2)$$

or explicitly [57]:

$$\hat{H}_{\text{eff}} = H_0 + \frac{\Omega^2}{\omega_0 - \omega_f} \left\{ 1 + \hat{S}_1^+ \hat{S}_2^- + \hat{S}_1^- \hat{S}_2^+ + (\hat{S}_1^z + \hat{S}_2^z) (2\hat{a}^\dagger \hat{a} + 1) \right\}.\quad (3)$$

In what follows, we present analytic solutions for the model Equations (1) and (3).

Our description of the problem is quite general. However, without loss of generality, we specify the values of the parameters relevant to the NV centers: Cantilever of mass $m = 6 \times 10^{-17}$ kg performs oscillations of the frequency $\frac{\omega_f}{2\pi} = 0.1 - 10$ MHz. The cavity mode $\frac{\omega_f}{2\pi} = 5$ MHz, and the coupling between cantilever and NV centers $\frac{\Omega}{2\pi} = 100$ kHz. The amplitude of the zero point fluctuations

$a_0 = \sqrt{\hbar/2m\omega_r} \approx 5 \times 10^{-3}$ m defines the characteristic energy scale of the problem $m\omega_r^2 a_0^2 \approx 10^{-9}$ J, and the time scale is of the order of microseconds.

3. The Analytical Solution

The model Equations (1) and (3) admit an exact analytical solution through the following ansatz:

$$|\phi(t)\rangle = \sum_{n=0}^{\infty} \{\Gamma_{n+1,eg}(t)|n+1, eg\rangle + \Gamma_{n+1,ge}(t)|n+1, ge\rangle + \Gamma_{n+2,gg}(t)|n+2, gg\rangle + \Gamma_{n,ee}(t)|n, ee\rangle\}. \quad (4)$$

Here, $|n\rangle$ is the state of the field with n phonons [49], and $|e\rangle \equiv |1\rangle$, $|g\rangle \equiv |0\rangle$ corresponds to the excited (ground) spin states of the NV centers. The explicit values of the coefficients $\Gamma_{n+1,eg}(t)$, $\Gamma_{n+1,ge}(t)$, $\Gamma_{n+2,gg}(t)$, $\Gamma_{n,ee}(t)$ are presented in the Appendix A. In what follows, we utilize these coefficients and construct the density matrix $\hat{\rho} = |\phi(t)\rangle\langle\phi(t)|$ corresponding to the model Equations (1) and (3).

4. The Invasive Measurement

In a magnetic resonance force microscopy experiment, the information about the state of the NV spin is read out through the magnetic tip. A measurement done on the spin A may perturb the state of the spin A directly and simultaneously may alter the state of the spin B indirectly through the quantized cantilever field. This is a case of non-local invasiveness and the non-local quantum witness. On the other hand, a measurement conducted directly on the phonon (cantilever) subsystem may influence the state of the NV spins directly (local witness). We start with studying the local witness.

4.1. Local Invasive Measurement

Suppose the measured phonon number is n . The measurement done on the subsystem f projects the wave function $|\phi(t)\rangle$ (see Equation (4)) to the post-measurement state:

$$|\Phi(t)\rangle = \frac{(\Pi_n^f \otimes I^s) |\phi(t)\rangle}{\sqrt{\langle\phi(t)| \Pi_n^f \otimes I^s |\phi(t)\rangle}}. \quad (5)$$

The post-measurement density matrix is given by:

$$\hat{\rho}_{\text{post}} = |\Phi(t)\rangle\langle\Phi(t)| = \frac{\Pi_n^f \hat{\rho} \Pi_n^f}{\text{Tr}(\Pi_n^f \hat{\rho} \Pi_n^f)}. \quad (6)$$

Here, I^s is the identity operator acting on the spin subsystem, and $\Pi_n^f = |n\rangle\langle n|$ is the phonon projection operator.

To quantify the quantum witness \mathcal{W} , we note that the system evolution is describable by an arbitrary positive, trace-preserving map $\hat{\mathcal{F}}$. The projector measurement operators for the spins we define as follows: $\Pi_{j\alpha}^s = |\alpha\rangle\langle\alpha|$. Here, $j = 1, 2$ enumerates the spins, and $\alpha = g, e$ stands for the ground and excited states. Then, for the (in the above sense) direct spin measurement probability, we deduce:

$$\mathcal{P}_{\hat{\rho}}^{j\alpha} = \text{Tr}\{\Pi_{j\alpha}^s \hat{\mathcal{F}}[\hat{\rho}]\}. \quad (7)$$

The indirect measurements probability reads:

$$\mathcal{Q}_{\hat{\rho}}^{j\alpha} = \text{Tr}\{\Pi_{j\alpha}^s \hat{\mathcal{F}}[\hat{\rho}_{\text{post}}]\}. \quad (8)$$

We note that in Equation (8), the first measurement (blind measurement) is done on the field subsystem. The trace preserving positive maps $\hat{\mathcal{F}}[\hat{\rho}] = \sum_{\alpha} \hat{L}_{\alpha} \hat{\rho} \hat{L}_{\alpha}^{\dagger}$ and $\hat{\mathcal{F}}[\hat{\rho}_{\text{post}}] = \sum_{\alpha} \hat{L}_{\alpha} \hat{\rho}_{\text{post}} \hat{L}_{\alpha}^{\dagger}$ are defined in terms of the Kraus operators $L_1 = \sqrt{\mu_1} |e\rangle\langle g|_1 \otimes |g\rangle\langle e|_2$ and $L_2 = \sqrt{\mu_2} |g\rangle\langle e|_1 \otimes |e\rangle\langle g|_2$, $\mu_1 + \mu_2 = 1$, see Appendix B.

For the system Equations (7) and (8), the quantum witness [11] is defined as follows:

$$\mathcal{W}_{\hat{\rho}}(j, \alpha) = \left| \mathcal{P}_{\hat{\rho}}^{j\alpha} - \mathcal{Q}_{\hat{\rho}}^{j\alpha} \right|. \quad (9)$$

Let the measured phonon number be m , then the post-measurement density matrix Equation (6) takes the form:

$$\begin{aligned} \hat{\rho}_{\text{post}} = Z^{-1} & \left\{ |\Gamma_{m,gg}(t)|^2 |m, gg\rangle \langle m, gg| + |\Gamma_{m,eg}(t)|^2 |m, eg\rangle \langle m, eg| + |\Gamma_{m,ge}(t)|^2 |m, ge\rangle \langle m, ge| \right. \\ & + |\Gamma_{m,ee}(t)|^2 |m, ee\rangle \langle m, ee| + \Gamma_{m,ge}(t) \Gamma_{m,eg}^*(t) |m, ge\rangle \langle m, eg| + \Gamma_{m,ge}(t) \Gamma_{m,gg}^*(t) |m, ge\rangle \langle m, gg| \\ & + \Gamma_{m,ge}(t) \Gamma_{m,ee}^*(t) |m, ge\rangle \langle m, ee| + \Gamma_{m,eg}(t) \Gamma_{m,gg}^*(t) |m, eg\rangle \langle m, gg| \\ & \left. + \Gamma_{m,eg}(t) \Gamma_{m,ee}^*(t) |m, eg\rangle \langle m, ee| + \Gamma_{m,gg}(t) \Gamma_{m,ee}^*(t) |m, gg\rangle \langle m, ee| + \text{h.c.} \right\}, \\ Z_m = & |\Gamma_{m,gg}(t)|^2 + |\Gamma_{m,eg}(t)|^2 + |\Gamma_{m,ge}(t)|^2 + |\Gamma_{m,ee}(t)|^2. \end{aligned} \quad (10)$$

The explicit analytical expressions of $\mathcal{P}_{\hat{\rho}}^{j\alpha}$, $\mathcal{Q}_{\hat{\rho}}^{j\alpha}$ are presented in the Appendix C.

After some calculations, for the measured phonon number m , we derive the analytical expression for the local quantum witness:

$$\mathcal{W}_{\hat{\rho}}^L(1, e) = \left| \mathcal{P}_{\hat{\rho}}^{1,e} - \mathcal{Q}_{\hat{\rho}}^{1,e} \right| = \mu_1 \left| \sum_{n=0}^{\infty} |\Gamma_{n,ge}(t)|^2 - \frac{|\Gamma_{m,ge}(t)|^2}{Z_m} \right|. \quad (11)$$

Here, $Z_m = 2 (|\Gamma_{m,ge}(t)|^2 + |\Gamma_{m,gg}(t)|^2)$.

For $u \gg 1$ (meaning the large mean phonon number), we use the saddle-point method and perform summation over the field states to get an analytical expression for the quantum witness in resonant case $\omega_0 = \omega_f$:

$$\begin{aligned} \mathcal{W}_{\hat{\rho}}^L(1, e) \approx \mu_1 u^2 & \left| \frac{[1 + \text{erf}(u/\sqrt{2})]}{4(2u^2 + 1)} \sin^2(\sqrt{4u^2 + 2\Omega t}) \right. \\ & \left. - \frac{\sin^2(\sqrt{4m + 2\Omega t})}{2u^2 \sin^2(\sqrt{4m + 2\Omega t}) + 4 \frac{1+2m}{(1-2m)^2} [m - 1 + m \cos(\sqrt{4m - 2\Omega t})]^2} \right| \end{aligned} \quad (12)$$

For the off-resonant Hamiltonian Equation (3), the $|n, gg\rangle$ state is decoupled. Therefore, one has to start from an excited state for the NV spins. Starting from the $|ge\rangle$ and a coherent phonon state, we obtain:

$$\mathcal{W}_{\hat{\rho}}^L(1, e) = \frac{\mu_1}{2} \left| \cos\left(\frac{2\Omega^2}{\omega_0 - \omega_f} t\right) \right|. \quad (13)$$

A plot of the quantum witness is presented in Figure 2. From Figure 2, we see that the saddle-point method smears out slow modulation of the amplitude of the quantum witness that we observe in the exact solution. The modulation of the witness strength amplitude is inherently a quantum effect related to the entanglement between the cavity field and NV centers. The saddle-point, which is valid for $u^2 \gg 1$, partially eliminates the entanglement effect. The witness is finite, but smaller than the maximum witness observed for the entangled states. The limit $u^2 \rightarrow \infty$ for the first term in Equation (12) leads to a fast oscillation between zero and 1/4, while the second term results in 1/2. In this case, the resonant Equation (12) and non-resonant Equation (13) results are of the same order.

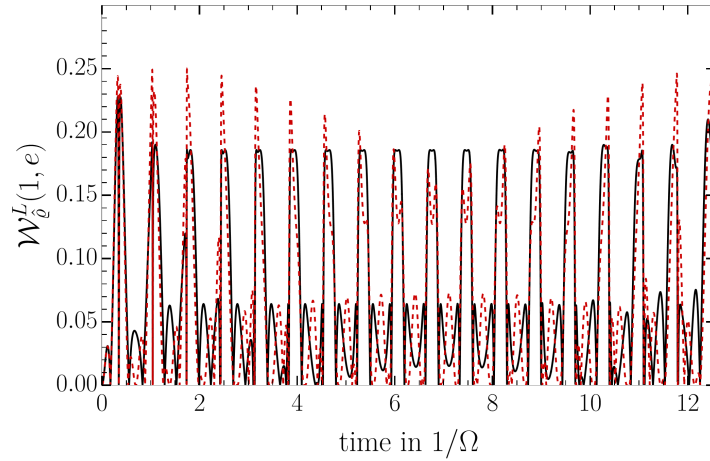


Figure 2. The quantum witness Equation (11) for the exact treatment (black) and the saddle-point approximation (red) for the initial condition $\Gamma_{n,gg}(0) = w_n$ with $w_n = \frac{u^n}{\sqrt{n!}} \exp(-u^2/2)$ and $u^2 = 20$ being the mean phonon number. The measured phonon number $m = 20$ and $\mu_1 = 0.5$.

4.2. Non-Local Invasive Measurement

The protocol of non-local invasive measurement is as follows: At the moment of time $t = \tau$, quantum measurement is done on the spin A through the positive operator valued measure (POVM) projection operator $\Pi_m^A = |m\rangle\langle m|$. Thus, the post-measurement density matrix has the form:

$$\hat{\rho}_S^{\text{post}} = \frac{\Pi_m^A \hat{\rho}(t) \Pi_m^A}{\text{Tr}(\Pi_m^A \hat{\rho}(t) \Pi_m^A)}. \quad (14)$$

Combining pre- and post-measurement density matrices, we find the density matrix at an arbitrary moment of time:

$$\hat{\rho}_1(t) = \Theta[\tau - t] \hat{\rho} + \Theta[t - \tau] \hat{\rho}_S^{\text{post}}. \quad (15)$$

Here, the explicit form of the post-measurement density matrix reads:

$$\hat{\rho}_S^{\text{post},e} = Z_e^{-1} \sum_{n,m=0}^{\infty} \left\{ \Gamma_{n+1,eg}(t) \Gamma_{m+1,eg}^*(t) |n+1, eg\rangle \langle m+1, eg| + \Gamma_{n+1,eg}(t) \Gamma_{m,ee}^*(t) |n+1, eg\rangle \langle m, ee| \right. \\ \left. + \Gamma_{n,ee}(t) \Gamma_{m+1,eg}^*(t) |n, ee\rangle \langle m+1, eg| + \Gamma_{n,ee}(t) \Gamma_{m,ee}^*(t) |n, ee\rangle \langle m, ee| \right\}, \quad (16)$$

$$Z_e = \sum_{n=0}^{\infty} \left(|\Gamma_{n,ee}(t)|^2 + |\Gamma_{n,eg}(t)|^2 \right),$$

$$\hat{\rho}_S^{\text{post},g} = Z_g^{-1} \sum_{n,m=0}^{\infty} \left\{ \Gamma_{n+1,ge}(t) \Gamma_{m+1,ge}^*(t) |n+1, ge\rangle \langle m+1, ge| \right. \\ \left. + \Gamma_{n+1,ge}(t) \Gamma_{m+2,gg}^*(t) |n+1, ge\rangle \langle m+2, gg| \right. \\ \left. + \Gamma_{n+2,gg}(t) \Gamma_{m+1,ge}^*(t) |n+2, gg\rangle \langle m+1, ge| \right. \\ \left. + \Gamma_{n+2,gg}(t) \Gamma_{m+2,gg}^*(t) |n+2, gg\rangle \langle m+2, gg| \right\}, \quad (17)$$

$$Z_g = \sum_{n=0}^{\infty} \left(|\Gamma_{n,gg}(t)|^2 + |\Gamma_{n,ge}(t)|^2 \right).$$

$\Theta[\dots]$ is the Heaviside step function.

The non-local quantum witness is defined as:

$$\mathcal{W}_{\hat{\rho}}^{\text{NL}}(1, e)_g = \left| \mathcal{P}_{\hat{\rho}_{\text{post},g}}^{1,e} - \mathcal{Q}_{\hat{\rho}_{\text{post},g}}^{1,e} \right|. \quad (18)$$

Using the saddle-point approximation for Equation (18) and taking into account Equation (12), we conclude that for the case $m \approx u^2$, $\mathcal{W}^{NL} \approx \mathcal{W}^L$ follows. Therefore, the invasiveness of the measurement is not enhanced in the case of indirect measurements.

5. Conclusions

The issue of the influence of a direct or indirect measurement on a composite quantum system can be quantified by the local and nonlocal quantum witness. For two effective quantum spins coupled to each other indirectly via the quantum oscillations of a cantilever, we derived an explicit expression for the local quantum witness \mathcal{W}^L that measures the invasiveness of a measurement done on the cantilever on the quantum states and hence on a subsequent measurement done on spins. The non-local quantum witness \mathcal{W}^{NL} delivers information on the reaction of the states of one spin when a measurement is performed on the other spin. Both spins are coupled only via the cantilever whose states can be steered into the classical regime. In both cases, invasiveness is the same $\mathcal{W}^L = \mathcal{W}^{NL}$. The obtained result confirms that the quantum channel mediates in both cases disturbances from the first to the second quantum spins. We analyzed the resonant solution comparing the exact result with the saddle-point method (Figure 2). We saw that the saddle-point method smeared out the slow modulation of the amplitude of the quantum witness that we observed in the exact solution. The modulation of the witness strength amplitude is inherently a quantum effect related to the entanglement between the cavity field and NV centers. The saddle-point, which is valid for $u^2 \gg 1$, partially eliminates the entanglement effect. The witness is finite, but smaller than the maximum witness observed for the entangled states.

Author Contributions: J.B. and L.C. conceived the idea and designed this research project. Calculations were performed by D.M. and D.S. All authors have read and agreed to the published version of the manuscript.

Funding: This research received no external funding.

Acknowledgments: We acknowledge financial support from DFG through SFB 762 and SFB TRR227. This work was supported by Shota Rustaveli National Science Foundation of Georgia (SRNSFG) (Grant Number FR-19-4049).

Conflicts of Interest: The authors declare no conflict of interest.

Appendix A

The time-dependent coefficients from ansatz Equation (4) in the resonant case of Hamiltonian Equation (1) follow the set of equations:

$$\begin{aligned}
 i \frac{d\Gamma_{gg,n+2}(t)}{dt} &= (n+1)\omega_f \Gamma_{gg,n+2}(t) + \Omega\sqrt{n+2} \{ \Gamma_{eg,n+1}(t) + \Gamma_{ge,n+1}(t) \}, \\
 i \frac{d\Gamma_{eg,n+1}(t)}{dt} &= (n+1)\omega_f \Gamma_{eg,n+1}(t) + \Omega \{ \sqrt{n+1} \Gamma_{ee,n}(t) + \sqrt{n+2} \Gamma_{gg,n+2}(t) \}, \\
 i \frac{d\Gamma_{ge,n+1}(t)}{dt} &= (n+1)\omega_f \Gamma_{ge,n+1}(t) + \Omega \{ \sqrt{n+1} \Gamma_{ee,n}(t) + \sqrt{n+2} \Gamma_{gg,n+2}(t) \}, \\
 i \frac{d\Gamma_{ee,n}(t)}{dt} &= (n+1)\omega_f \Gamma_{ee,n}(t) + \Omega\sqrt{n+1} \{ \Gamma_{ge,n}(t) + \Gamma_{eg,n+2}(t) \}.
 \end{aligned} \tag{A1}$$

For Equation (A1), we adopt the initial conditions $\Gamma_{gg,n+2}(0) = w_{n+2}$ and $\Gamma_{eg,n+1}(0) = \Gamma_{ge,n+1}(0) = \Gamma_{ee,n}(0) = 0$ and obtain the solution:

$$\begin{aligned}
\Gamma_{gg,n+2}(t) &= e^{-i(n+1)\omega_f t} \frac{(n+2) \cos(\sqrt{4n+6}\Omega t) + n+1}{2n+3} w_{n+2}, \\
\Gamma_{ee,n}(t) &= e^{-i(n+1)\omega_f t} \frac{\sqrt{(n+1)(n+2)} [\cos(\sqrt{4n+6}\Omega t) - 1]}{2n+3} w_{n+2}, \\
\Gamma_{eg,n+1}(t) = \Gamma_{ge,n+1}(t) &= e^{-i(n+1)\omega_f t} \frac{i\sqrt{n+2} \sin(\sqrt{4n+6}\Omega t)}{\sqrt{4n+6}} w_{n+2}.
\end{aligned} \tag{A2}$$

For the initial state of the phonon subsystem, we take $w_n = \frac{u^n}{\sqrt{n!}} \exp(-u^2/2)$ where u^2 is the mean phonon number.

We note that an effective interaction between NV spins is obtained through perturbation theory. The relation we use in what follows $|\omega_0 - \omega_f| = \Omega$ defines the lower bounds of detuning allowed by perturbation theory (the maximal interaction strength). For smaller detuning $|\omega_0 - \omega_f| < \Omega$, the approximation is not valid. In the non-resonant case $|\omega_0 - \omega_f| > \Omega$, the solution is different from Equation (A2). For the Hamiltonian Equation (3), we utilize the ansatz Equation (4) and deduce the set of equations:

$$\begin{aligned}
i \frac{d\Gamma_{gg,n+2}(t)}{dt} &= ((n+2)\omega_f - \omega_0 - (2n+4)J) \Gamma_{gg,n+2}(t), \\
i \frac{d\Gamma_{eg,n+1}(t)}{dt} &= ((n+1)\omega_f + J) \Gamma_{eg,n+1}(t) + J\Gamma_{ge,n+1}(t), \\
i \frac{d\Gamma_{ge,n+1}(t)}{dt} &= ((n+1)\omega_f + J) \Gamma_{ge,n+1}(t) + J\Gamma_{eg,n+1}(t), \\
i \frac{d\Gamma_{ee,n}(t)}{dt} &= (n\omega_f + \omega_0 + (2n+2)J) \Gamma_{ee,n}(t).
\end{aligned} \tag{A3}$$

The set of equations (A3) leads to the non-resonant solution Equation (13), which in the limit of large u is of the same order as the resonant solution Equation (12).

Appendix B

The trace-preserving Kraus channels are:

$$\hat{\mathcal{F}}[\hat{\rho}] = \sum_{n=0}^{\infty} \left\{ \mu_1 |\Gamma_{n+1,ge}(t)|^2 |n+1, eg\rangle \langle n+1, eg| + \mu_2 |\Gamma_{n+1,eg}(t)|^2 |n+1, ge\rangle \langle n+1, ge| \right\}, \tag{A4}$$

$$\hat{\mathcal{F}}[\hat{\rho}_{\text{post}}] = Z_m^{-1} \left(\mu_2 |\Gamma_{m,eg}(t)|^2 |m, ge\rangle \langle m, ge| + \mu_1 |\Gamma_{m,ge}(t)|^2 |m, eg\rangle \langle m, eg| \right), \tag{A5}$$

$$\hat{\mathcal{F}}[\hat{\rho}_S^{\text{post},e}] = \mu_2 Z_e^{-1} \sum_{n,m=0}^{\infty} \Gamma_{n+1,eg}(t) \Gamma_{m+1,ge}^*(t) |n+1, ge\rangle \langle m+1, ge|, \tag{A6}$$

$$\hat{\mathcal{F}}[\hat{\rho}_S^{\text{post},g}] = \mu_1 Z_g^{-1} \sum_{n,m=0}^{\infty} \Gamma_{n+1,ge}(t) \Gamma_{m+1,eg}^*(t) |n+1, ge\rangle \langle m+1, eg|. \tag{A7}$$

Appendix C

The direct measurement probabilities are:

$$\begin{aligned}
\mathcal{P}_{\hat{\rho}}^{1,e} = \mathcal{P}_{\hat{\rho}}^{2,g} &= \mu_1 \sum_{n=0}^{\infty} |\Gamma_{n,ge}(t)|^2, \\
\mathcal{P}_{\hat{\rho}}^{2,e} = \mathcal{P}_{\hat{\rho}}^{1,g} &= \mu_2 \sum_{n=0}^{\infty} |\Gamma_{n,eg}(t)|^2
\end{aligned} \tag{A8}$$

The indirect (blind) measurement results (measurement results are discarded):

$$\begin{aligned} Q_{\hat{q}}^{1,e} = Q_{\hat{q}}^{2,g} &= Z_m^{-1} \mu_1 |\Gamma_{m,ge}(t)|^2, \\ Q_{\hat{q}}^{2,e} = Q_{\hat{q}}^{1,g} &= Z_m^{-1} \mu_2 |\Gamma_{m,eg}(t)|^2. \end{aligned} \quad (\text{A9})$$

$$\begin{aligned} Q_{\hat{q}_{\text{post},g}}^{2,e} = Q_{\hat{q}_{\text{post},g}}^{1,g} &= 0, \\ Q_{\hat{q}_{\text{post},g}}^{1,e} = Q_{\hat{q}_{\text{post},g}}^{2,g} &= Z_g^{-1} \mu_1 \sum_{n=0}^{\infty} |\Gamma_{n,ge}(t)|^2. \end{aligned} \quad (\text{A10})$$

$$\begin{aligned} Q_{\hat{q}_{\text{post},e}}^{1,e} = Q_{\hat{q}_{\text{post},e}}^{2,g} &= 0, \\ Q_{\hat{q}_{\text{post},e}}^{2,e} = Q_{\hat{q}_{\text{post},e}}^{1,g} &= Z_e^{-1} \mu_2 \sum_{n=0}^{\infty} |\Gamma_{n,eg}(t)|^2. \end{aligned} \quad (\text{A11})$$

References

1. Emary, C.; Lambert, N.; Nori, F. Leggett–garg inequalities. *Rep. Prog. Phys.* **2013**, *77*, 016001. [\[CrossRef\]](#)
2. Hoffmann, J.; Spee, C.; Gühne, O.; Budroni, C. Structure of temporal correlations of a qubit. *New J. Phys.* **2018**, *20*, 102001. [\[CrossRef\]](#)
3. Kofler, J.; Brukner, Č. Condition for macroscopic realism beyond the Leggett-Garg inequalities. *Phys. Rev. A* **2013**, *87*, 052115. [\[CrossRef\]](#)
4. Song, X.K.; Huang, Y.; Ling, J.; Yung, M.H. Quantifying quantum coherence in experimentally observed neutrino oscillations. *Phys. Rev. A* **2018**, *98*, 050302. [\[CrossRef\]](#)
5. Halliwell, J.; Mawby, C. Fine’s theorem for Leggett-Garg tests with an arbitrary number of measurement times. *Phys. Rev. A* **2019**, *100*, 042103. [\[CrossRef\]](#)
6. Naikoo, J.; Banerjee, S.; Jayannavar, A.M. Violation of Leggett-Garg-type inequalities in a driven two-level atom interacting with a squeezed thermal reservoir. *Phys. Rev. A* **2019**, *100*, 062132. [\[CrossRef\]](#)
7. Nikitin, N.; Toms, K. Wigner inequalities for testing the hypothesis of realism and concepts of macroscopic and local realism. *Phys. Rev. A* **2019**, *100*, 062314. [\[CrossRef\]](#)
8. Williams, N.S.; Jordan, A.N. Weak values and the Leggett-Garg inequality in solid-state qubits. *Phys. Rev. Lett.* **2008**, *100*, 026804. [\[CrossRef\]](#)
9. Robens, C.; Alt, W.; Meschede, D.; Emary, C.; Alberti, A. Ideal negative measurements in quantum walks disprove theories based on classical trajectories. *Phys. Rev. X* **2015**, *5*, 011003. [\[CrossRef\]](#)
10. Skinner, B.; Ruhman, J.; Nahum, A. Measurement-induced phase transitions in the dynamics of entanglement. *Phys. Rev. X* **2019**, *9*, 031009. [\[CrossRef\]](#)
11. Leggett, A.J.; Garg, A. Quantum mechanics versus macroscopic realism: Is the flux there when nobody looks? *Phys. Rev. Lett.* **1985**, *54*, 857. [\[CrossRef\]](#) [\[PubMed\]](#)
12. Schild, G.; Emary, C. Maximum violations of the quantum-witness equality. *Phys. Rev. A* **2015**, *92*, 032101. [\[CrossRef\]](#)
13. Wang, K.; Knee, G.C.; Zhan, X.; Bian, Z.; Li, J.; Xue, P. Optimal experimental demonstration of error-tolerant quantum witnesses. *Phys. Rev. A* **2017**, *95*, 032122. [\[CrossRef\]](#)
14. Avis, D.; Hayden, P.; Wilde, M.M. Leggett-Garg inequalities and the geometry of the cut polytope. *Phys. Rev. A* **2010**, *82*, 030102. [\[CrossRef\]](#)
15. Li, C.M.; Lambert, N.; Chen, Y.N.; Chen, G.Y.; Nori, F. Witnessing quantum coherence: From solid-state to biological systems. *Sci. Rep.* **2012**, *2*, 885. [\[CrossRef\]](#)
16. Dong, Y.; Chen, X.D.; Guo, G.C.; Sun, F.W. Robust scalable architecture for a hybrid spin-mechanical quantum entanglement system. *Phys. Rev. B* **2019**, *100*, 214103. [\[CrossRef\]](#)
17. Jin, Z.; Su, S.; Zhang, S. Preparation of a steady entangled state of two nitrogen-vacancy centers by simultaneously utilizing two dissipative factors. *Phys. Rev. A* **2019**, *100*, 052332. [\[CrossRef\]](#)
18. Tchegotareva, A.; Hermans, S.L.; Humphreys, P.C.; Voigt, D.; Harmsma, P.J.; Cheng, L.K.; Verlaan, A.L.; Dijkhuizen, N.; De Jong, W.; Dréau, A.; et al. Entanglement between a diamond spin qubit and a photonic time-bin qubit at telecom wavelength. *Phys. Rev. Lett.* **2019**, *123*, 063601. [\[CrossRef\]](#)

19. Ma, Y.H.; Ding, Q.Z.; Wu, E. Entanglement of two nitrogen-vacancy ensembles via a nanotube. *Phys. Rev. A* **2020**, *101*, 022311. [[CrossRef](#)]
20. Qiao, Y.F.; Li, H.Z.; Dong, X.L.; Chen, J.Q.; Zhou, Y.; Li, P.B. Phononic-waveguide-assisted steady-state entanglement of silicon-vacancy centers. *Phys. Rev. A* **2020**, *101*, 042313. [[CrossRef](#)]
21. Roszak, K.; Kwiatkowski, D.; Cywiński, Ł. How to detect qubit-environment entanglement generated during qubit dephasing. *Phys. Rev. A* **2019**, *100*, 022318. [[CrossRef](#)]
22. Chen, X.Y.; Yin, Z.q. Universal quantum gates between nitrogen-vacancy centers in a levitated nanodiamond. *Phys. Rev. A* **2019**, *99*, 022319. [[CrossRef](#)]
23. Singh, A.; Chotorlishvili, L.; Srivastava, S.; Tralle, I.; Toklikishvili, Z.; Berakdar, J.; Mishra, S. Generation of coherence in an exactly solvable nonlinear nanomechanical system. *Phys. Rev. B* **2020**, *101*, 104311. [[CrossRef](#)]
24. Naik, A.K.; Hanay, M.; Hiebert, W.; Feng, X.; Roukes, M.L. Towards single-molecule nanomechanical mass spectrometry. *Nat. Nanotechnol.* **2009**, *4*, 445–450. [[CrossRef](#)]
25. O'Connell, A.D.; Hofheinz, M.; Ansmann, M.; Bialczak, R.C.; Lenander, M.; Lucero, E.; Neeley, M.; Sank, D.; Wang, H.; Weides, M.; et al. Quantum ground state and single-phonon control of a mechanical resonator. *Nature* **2010**, *464*, 697–703. [[CrossRef](#)]
26. Safavi-Naeini, A.H.; Alegre, T.M.; Chan, J.; Eichenfield, M.; Winger, M.; Lin, Q.; Hill, J.T.; Chang, D.E.; Painter, O. Electromagnetically induced transparency and slow light with optomechanics. *Nature* **2011**, *472*, 69–73. [[CrossRef](#)]
27. Stannigel, K.; Rabl, P.; Sørensen, A.S.; Zoller, P.; Lukin, M.D. Optomechanical transducers for long-distance quantum communication. *Phys. Rev. Lett.* **2010**, *105*, 220501. [[CrossRef](#)]
28. Safavi-Naeini, A.H.; Painter, O. Proposal for an optomechanical traveling wave phonon–photon translator. *New J. Phys.* **2011**, *13*, 013017. [[CrossRef](#)]
29. Camerer, S.; Korppi, M.; Jöckel, A.; Hunger, D.; Hänsch, T.W.; Treutlein, P. Realization of an optomechanical interface between ultracold atoms and a membrane. *Phys. Rev. Lett.* **2011**, *107*, 223001. [[CrossRef](#)]
30. Eichenfield, M.; Chan, J.; Camacho, R.M.; Vahala, K.J.; Painter, O. Optomechanical crystals. *Nature* **2009**, *462*, 78–82. [[CrossRef](#)]
31. Safavi-Naeini, A.H.; Chan, J.; Hill, J.T.; Alegre, T.P.M.; Krause, A.; Painter, O. Observation of quantum motion of a nanomechanical resonator. *Phys. Rev. Lett.* **2012**, *108*, 033602. [[CrossRef](#)] [[PubMed](#)]
32. Brahm, N.; Botter, T.; Schreppler, S.; Brooks, D.W.; Stamper-Kurn, D.M. Optical detection of the quantization of collective atomic motion. *Phys. Rev. Lett.* **2012**, *108*, 133601. [[CrossRef](#)]
33. Nunnenkamp, A.; Børkje, K.; Girvin, S. Cooling in the single-photon strong-coupling regime of cavity optomechanics. *Phys. Rev. A* **2012**, *85*, 051803. [[CrossRef](#)]
34. Khalili, F.Y.; Miao, H.; Yang, H.; Safavi-Naeini, A.H.; Painter, O.; Chen, Y. Quantum back-action in measurements of zero-point mechanical oscillations. *Phys. Rev. A* **2012**, *86*, 033840. [[CrossRef](#)]
35. Meaney, C.P.; McKenzie, R.H.; Milburn, G. Quantum entanglement between a nonlinear nanomechanical resonator and a microwave field. *Phys. Rev. E* **2011**, *83*, 056202. [[CrossRef](#)] [[PubMed](#)]
36. Atalaya, J.; Isacsson, A.; Dykman, M. Diffusion-induced dephasing in nanomechanical resonators. *Phys. Rev. B* **2011**, *83*, 045419. [[CrossRef](#)]
37. Rabl, P. Cooling of mechanical motion with a two-level system: The high-temperature regime. *Phys. Rev. B* **2010**, *82*, 165320. [[CrossRef](#)]
38. Prants, S. A group-theoretical approach to study atomic motion in a laser field. *J. Phys. A Math. Theor.* **2011**, *44*, 265101. [[CrossRef](#)]
39. Chotorlishvili, L.; Toklikishvili, Z.; Berakdar, J. Thermal entanglement and efficiency of the quantum Otto cycle for the su(1, 1) Tavis–Cummings system. *J. Phys. A Math. Theor.* **2011**, *44*, 165303. [[CrossRef](#)]
40. Chotorlishvili, L.; Schwab, P.; Toklikishvili, Z.; Skrinnikov, V. Entanglement sudden death and influence of the dynamical Stark shift for two Tavis–Cummings atoms. *Phys. Lett. A* **2010**, *374*, 1642–1647. [[CrossRef](#)]
41. Ludwig, M.; Hammerer, K.; Marquardt, F. Entanglement of mechanical oscillators coupled to a nonequilibrium environment. *Phys. Rev. A* **2010**, *82*, 012333. [[CrossRef](#)]
42. Schmidt, T.L.; Børkje, K.; Bruder, C.; Trauzettel, B. Detection of qubit-oscillator entanglement in nanoelectromechanical systems. *Phys. Rev. Lett.* **2010**, *104*, 177205. [[CrossRef](#)] [[PubMed](#)]
43. Karabalin, R.; Cross, M.; Roukes, M. Nonlinear dynamics and chaos in two coupled nanomechanical resonators. *Phys. Rev. B* **2009**, *79*, 165309. [[CrossRef](#)]

44. Chotorlishvili, L.; Ugulava, A.; Mchedlishvili, G.; Komnik, A.; Wimberger, S.; Berakdar, J. Nonlinear dynamics of two coupled nano-electromechanical resonators. *J. Phys. B At. Mol. Opt. Phys.* **2011**, *44*, 215402. [[CrossRef](#)]
45. Liu, Y.x.; Miranowicz, A.; Gao, Y.B.; Bajer, J.c.v.; Sun, C.P.; Nori, F. Qubit-induced phonon blockade as a signature of quantum behavior in nanomechanical resonators. *Phys. Rev. A* **2010**, *82*, 032101. doi:10.1103/PhysRevA.82.032101. [[CrossRef](#)]
46. Shevchenko, S.; Ashhab, S.; Nori, F. Landau–Zener–Stückelberg interferometry. *Phys. Rep.* **2010**, *492*, 1–30. doi:10.1016/j.physrep.2010.03.002. [[CrossRef](#)]
47. Zueco, D.; Reuther, G.M.; Kohler, S.; Hänggi, P. Qubit-oscillator dynamics in the dispersive regime: Analytical theory beyond the rotating-wave approximation. *Phys. Rev. A* **2009**, *80*, 033846. doi:10.1103/PhysRevA.80.033846. [[CrossRef](#)]
48. Cohen, G.Z.; Di Ventra, M. Reading, writing, and squeezing the entangled states of two nanomechanical resonators coupled to a SQUID. *Phys. Rev. B* **2013**, *87*, 014513. doi:10.1103/PhysRevB.87.014513. [[CrossRef](#)]
49. Rabl, P.; Cappellaro, P.; Dutt, M.V.G.; Jiang, L.; Maze, J.R.; Lukin, M.D. Strong magnetic coupling between an electronic spin qubit and a mechanical resonator. *Phys. Rev. B* **2009**, *79*, 041302. doi:10.1103/PhysRevB.79.041302. [[CrossRef](#)]
50. Zhou, L.g.; Wei, L.F.; Gao, M.; Wang, X.b. Strong coupling between two distant electronic spins via a nanomechanical resonator. *Phys. Rev. A* **2010**, *81*, 042323. doi:10.1103/PhysRevA.81.042323. [[CrossRef](#)]
51. Chotorlishvili, L.; Sander, D.; Sukhov, A.; Dugaev, V.; Vieira, V.R.; Komnik, A.; Berakdar, J. Entanglement between nitrogen vacancy spins in diamond controlled by a nanomechanical resonator. *Phys. Rev. B* **2013**, *88*, 085201. doi:10.1103/PhysRevB.88.085201. [[CrossRef](#)]
52. Rugar, D.; Budakian, R.; Mamin, H.J.; Chui, B.W. Single spin detection by magnetic resonance force microscopy. *Nature* **2004**, *430*, 329. [[CrossRef](#)] [[PubMed](#)]
53. Treutlein, P. A Single Spin Feels the Vibrations. *Science* **2012**, *335*, 1584. [[CrossRef](#)] [[PubMed](#)]
54. Melkikh, A.V. Quantum information and microscopic measuring instruments. *Commun. Theor. Phys.* **2019**, *72*, 015101. [[CrossRef](#)]
55. Melkikh, A.V. Nonlinearity of quantum mechanics and solution of the problem of wave function collapse. *Commun. Theor. Phys.* **2015**, *64*, 47. [[CrossRef](#)]
56. Fröhlich, H. Quantum information and microscopic measuring instruments. *Proc. R. Soc. Lond.* **1952**, *215*, 291.
57. Trif, M.; Golovach, V.N.; Loss, D. Spin dynamics in InAs nanowire quantum dots coupled to a transmission line. *Phys. Rev. B* **2008**, *77*, 045434. doi:10.1103/PhysRevB.77.045434. [[CrossRef](#)]



© 2020 by the authors. Licensee MDPI, Basel, Switzerland. This article is an open access article distributed under the terms and conditions of the Creative Commons Attribution (CC BY) license (<http://creativecommons.org/licenses/by/4.0/>).